



HAL
open science

End-to-end wind turbine design under uncertainties : a practical example

N. K. Dimitrov, M. Kelly, M. Mcwilliam, Martin Guiton, Alexis Cousin, Pierre-Antoine Joulin, Maria Laura Mayol, Miguel Munoz-Zuniga, Lucas Franceschini, A. Lovera, et al.

► To cite this version:

N. K. Dimitrov, M. Kelly, M. Mcwilliam, Martin Guiton, Alexis Cousin, et al.. End-to-end wind turbine design under uncertainties : a practical example. *Journal of Physics: Conference Series*, 2024, 2767 (8), pp.082017. 10.1088/1742-6596/2767/8/082017 . hal-04652746

HAL Id: hal-04652746

<https://ifp.hal.science/hal-04652746>

Submitted on 18 Jul 2024

HAL is a multi-disciplinary open access archive for the deposit and dissemination of scientific research documents, whether they are published or not. The documents may come from teaching and research institutions in France or abroad, or from public or private research centers.

L'archive ouverte pluridisciplinaire **HAL**, est destinée au dépôt et à la diffusion de documents scientifiques de niveau recherche, publiés ou non, émanant des établissements d'enseignement et de recherche français ou étrangers, des laboratoires publics ou privés.



Distributed under a Creative Commons Attribution 4.0 International License

PAPER • OPEN ACCESS

End-to-end wind turbine design under uncertainties: a practical example

To cite this article: NK Dimitrov *et al* 2024 *J. Phys.: Conf. Ser.* **2767** 082017

View the [article online](#) for updates and enhancements.

You may also like

- [Using intrusive approaches as a step towards accounting for stochasticity in wind turbine design](#)
E. Branlard, C. Frontin, J. Maack et al.
- [Towards a general tool chain integration platform for multi-disciplinary analysis and optimization in wind energy](#)
Ju Feng and Jens Nørkær Sørensen
- [GNN-based surrogate modeling for collection systems costs](#)
M Souza De Alencar, T Göçmen and N A Cutululis

PRIMETM
PACIFIC RIM MEETING
ON ELECTROCHEMICAL
AND SOLID STATE SCIENCE

HONOLULU, HI
October 6-11, 2024

Joint International Meeting of
The Electrochemical Society of Japan (ECSJ)
The Korean Electrochemical Society (KECS)
The Electrochemical Society (ECS)

Early Registration Deadline:
September 3, 2024

**MAKE YOUR PLANS
NOW!**

End-to-end wind turbine design under uncertainties: a practical example

NK Dimitrov¹, M Kelly¹, M. McWilliam¹, M Guiton², A Cousin²,
PA Joulin², ML Mayol², M Munoz-Zuniga², L Franceschini², A
Lovera³, E Fekhari³, E Ardillon³, C Peyrard³, M
Bakhoday-Paskyabi⁴, S Marelli⁵, S Schar⁵, E Vanem⁶, C Agrell⁶, O
Gramstad⁶, H Wang⁶

¹Technical University of Denmark, DTU Wind and Energy Systems, Roskilde, Denmark

²IFP Energies nouvelles, Lyon and Rueil-Malmaison, France

³Electricite De France, Paris, France

⁴University of Bergen, Geophysical Institute, Bergen, Norway

⁵ETH Zurich, Department of Civil Engineering, Zurich, Switzerland

⁶Det Norske Veritas, Høvik, Norway

E-mail: nkdi@dtu.dk

Abstract. This paper illustrates the process of design under uncertainty on a practical case study of an offshore wind farm. We document the entire process through selection and quantification of relevant uncertainties, definition of probabilistic limit states, reliability computation algorithms, as well as illustrating the impacts of the analysis through a design utilization study. The brief introduction in this study draws information and summarizes outcomes from the extensive works that took part within the EU H2020 HIPERWIND project. The results from the study show that significant material savings can be achieved by introducing probabilistic design methodologies, and particularly with the help of an integrated modelling approach where the entire structure (turbine, tower & foundation) is considered as a whole.

1. Introduction

It is well known that the structural integrity of engineering structures is affected by various uncertainties. This effect is especially pronounced for wind turbines due to the highly variable environmental conditions in which they operate. In the classical wind turbine design process, the effects of uncertainty in environmental conditions, material strength, and modelling accuracy are accounted for by the application of safety factors. As an alternative, the uncertainty information can be fully integrated into the design by employing probabilistic models and propagating the uncertainties through the entire modelling chain, carrying out a so-called probabilistic design or design under uncertainty. In addition to a much more complete understanding of uncertainty, this approach may provide cost savings by reducing conservatism wherever the uncertainty can be reduced. Recently, IEC TS 61400-9 ED1 [1] has provided a formal framework for the application of probabilistic design to wind energy. Nevertheless, probabilistic design is rarely carried out in practice due to the added complexity and the difficulty in assessing the associated uncertainties. Aiming to demonstrate the impact of probabilistic design techniques, the EU



Horizon2020 HIPERWIND project [2] develops, improves and tests methodologies that can showcase the entire process of design under uncertainty for concrete use cases.

The primary goal of this study is to provide a brief practical demonstration of how probabilistic methodologies can be used to assess the design integrity and reduce the material usage while ensuring sufficient reliability. The paper illustrates the approach on an use case of a fixed-bottom offshore wind farm with monopile foundations. Throughout this process, we also aim to show 1) what are the main sources of uncertainty and how they can be quantified throughout the wind turbine design modelling chain, 2) how the uncertainty information is integrated in the wind turbine design process, and 3) what are the potential benefits and challenges with design under uncertainty.

2. Methodology

According to standard practices, the adequacy of a design solution is assessed through formulating and evaluating a limit state function $g(\mathbf{X})$, where \mathbf{X} represents a set of (potentially stochastic) environmental conditions and design variables. For a given design scenario, $g(\mathbf{X}) > 0$ points to survival of the structure, while $g(\mathbf{X}) \leq 0$ represents failure. Often the equation is divided in two terms, $g(\mathbf{X}) = R(\mathbf{X}) - S(\mathbf{X})$, where $S(\mathbf{X})$ represents the loads (actions) affecting the structure, while $R(\mathbf{X})$ represents the resistance of the structure - i.e., its ability to withstand such loads. With a deterministic design approach, a number of design scenarios are evaluated under varying environmental conditions and specific critical events, see e.g. IEC61400-1 [3]. Any sources of uncertainty besides the external conditions are accounted for by introducing safety factors in the limit state equation. A design solution is deemed adequate if the resistance is greater than the loading for all design scenarios considered, i.e., $(1/\gamma_m)R - \gamma_f S > 0$, where γ_m and γ_f are safety factors for material strength and loads, respectively.

In contrast, a probabilistic design procedure will explicitly take stochasticity and uncertainties into account by introducing them as components of \mathbf{X} which in this case is a random vector with joint probability distribution $f_{\mathbf{X}}(\mathbf{x})$. Rather than involving safety factors, the adequacy of the design is determined by assessing whether the total probability of failure, $p_f = P(g(\mathbf{X}) \leq 0)$, is sufficiently low. Computing this failure probability is the main subject of structural reliability analysis [4]. This methodology increases the complexity of the analysis with two specific hurdles: 1) defining a probabilistic limit state that takes all relevant uncertainties (epistemic and aleatory) in the modelling chain into account, and properly quantifying them, which may require significant amounts of data and modelling efforts, and 2) dealing with distributions rather than single samples leads to significantly (up to orders of magnitude) higher computational budgets, thus relying on simplifying assumptions and greedy sampling techniques. The present study shows an example of how these challenges are solved for a concrete case study.

2.1. Joint distribution definition

We distinguish between three types of stochastic variables included in $\mathbf{X} = \{\mathbf{V}, \mathbf{Z}, \mathbf{U}\}$: 1) environmental random variables constituting a random vector \mathbf{V} , 2) random variables \mathbf{Z} , called system variables, independent from \mathbf{V} , and 3) model uncertainty variables \mathbf{U} . The variables in \mathbf{Z} represent properties which affect the structural behavior such as e.g., material stiffness. Each structure under consideration (e.g., a wind turbine) is considered to represent a single realization from the probability distribution of \mathbf{Z} . On the other hand, the variables in \mathbf{V} are external to the structure and represent conditions that will be continuously changing over the lifetime of the structure, such as environmental parameters. As a result, the distribution of \mathbf{V} needs to be determined and sampled with respect to a short-term reference period. In the present study we use a 10-minute reference period which is the broadly accepted standard for wind measurements. Figure 1 shows an overview of the elements of the modelling chain considered by our work, and the associated uncertainties. In order to reduce the problem to a manageable extent, the

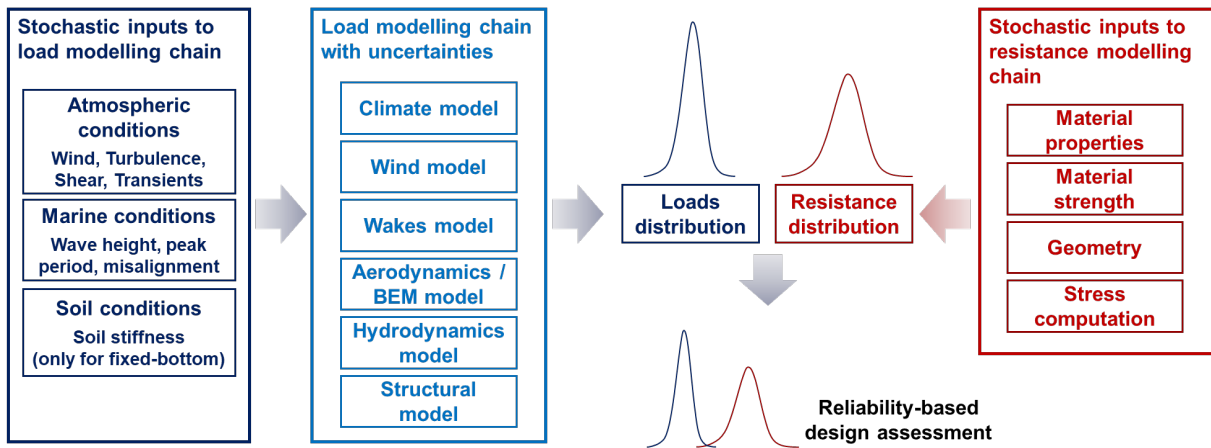


Figure 1: Overview of the random external variables and model uncertainties considered in the analysis.

primary focus is on the loading side of the limit state equation. The material resistance is considered probabilistic (included in \mathbf{Z}), but no concrete efforts are made for refining the models or quantifying the uncertainties on this side of the equation. Instead, generic values are taken from literature (see Section 3.3). As shown in Figure 1, the load-related random variables can be broadly grouped in two categories. The first category is the stochastic inputs to the load modelling chain, which contains a combination of aleatory uncertainties (e.g. due to random variation in the environmental conditions \mathbf{V} , and the soil stiffness, which is considered part of \mathbf{Z} because it affects the structural behavior), as well as some epistemic uncertainties due to, e.g., measurement uncertainty. The second category, uncertainties in the modelling chain, comprises only epistemic uncertainties affecting the models that are used (referred to as variables \mathbf{U}).

2.2. Limit state definition

We consider two limit states: Fatigue (FLS) and Ultimate (ULS). While these are subjected to separate reliability calculations, they both follow the variable selection and categorization as presented in Figure 1. A major difference between the limit states is that ULS considers the probability of a single excursion (loads exceeding resistance) at any time, while FLS considers the probability that the accumulated loading cycles will exceed the fatigue capacity. This leads to differences in the way \mathbf{V} is treated, where ULS uses directly the joint probability of any given combination of values in \mathbf{V} , while in the FLS case each evaluation of the limit state function requires a numerical integration over the joint probability distribution of \mathbf{V} .

For the ULS, g is defined in equation (1) where ΔT represents the duration of the considered period, t is the time variable, QoI is some time-dependent quantity of interest such as the stress at some location of the structure and ρ is a threshold such as the yield strength.

$$g(\mathbf{V}, \mathbf{Z}, \mathbf{U}) = \rho(\mathbf{Z}) - \max_{t \in [0, \Delta T]} QoI(t, \mathbf{V}, \mathbf{Z}, \mathbf{U}) \quad (1)$$

Hence, failure occurs if the quantity of interest exceeds the threshold over the time period. Note that for a given set of environmental conditions \mathbf{V} , structure parameters \mathbf{Z} and model parameters \mathbf{U} , $QoI(t, \mathbf{V}, \mathbf{Z}, \mathbf{U})$ is still random since it depends also on the short-term variation represented with random realizations of wind and wave time series in the simulations.

As discussed, the FLS case involves computing the total fatigue damage accumulated in a critical point of the structure and conditioned on the environmental variables for a given \mathbf{Z}

realization. This is denoted as global damage, D_{global} and is computed as a weighted sum (expectation) over \mathbf{V} : $D_{global} = E_{\mathbf{V}}[D(\mathbf{V}, \mathbf{Z}, \mathbf{U})]$ where $D(\mathbf{V}, \mathbf{Z}, \mathbf{U})$ represents marginal fatigue damage for a given 10-minute combination of conditions \mathbf{v} and for given realizations of system variables \mathbf{z} and model uncertainties \mathbf{u} . Using this notation, the FLS limit state equation becomes

$$g(\mathbf{V}, \mathbf{Z}, \mathbf{U}) = D_{CR} - D_{global}(\mathbf{V}, \mathbf{Z}, \mathbf{U}) \quad (2)$$

where $D_{CR} \in \mathbf{Z}$ stands for the critical damage leading to fatigue-induced failure of the structure.

2.3. Use case description

The proposed methodologies are applied on the use case of the Teesside offshore wind farm, which has been operated by EDF since 2014. The site consists of 27 SWT2.3-93 wind turbines installed on monopile foundations. There are approximately 5 years of SCADA and met mast data available to the study team, as well as a wave buoy. The reliability assessment is performed at the tower base, where the structural resistance is evaluated in terms of Von Mises stresses in an isotropic material (steel).

The following two sections describe in details the uncertainty modelling and the reliability computation tasks, respectively.

3. Uncertainty and distribution modelling

3.1. Environmental distributions

The distributions of 10-minute environmental conditions statistics were established based on the site measurements as described in Section 2.3. A total of six environmental variables were considered: wind mean speed U , turbulence σ_U , significant wave height H_s , wave peak period T_P , wind direction θ , and wave direction α . A conditional distribution model was fit to all variables, with more details including distribution parameters given in [23, 24]. A significant source of uncertainty was found in the conditional distribution models, for combinations of extreme conditions (environmental contours). The uncertainty is partly due to lack of data (only few years available), but is also very much affected by arbitrary choices of distribution models that can be made. This situation is illustrated in the left hand side of Figure 2. The issue can however be reduced by using reanalysis data and data from multi-scale model simulations, as shown in recent studies [9, 10].

Special attention was paid to detecting and describing load-inducing transient events, via flow acceleration statistics. Such statistics were not available at Teesside, so the 17 years of offshore data analyzed from Høvsøre [7, 8] were applied to Teesside (open sea directions). Extreme accelerations are not necessarily turbulence, and do not correlate well with 10-minute U or σ_u . A constrained turbulence simulation approach was used to reproduce an ensemble of P_{99} of accelerations, showing that there are cases where the IEC can under-predict certain loads [6]. These transient events were integrated in the reliability analysis by using the synthetic gust function

$$U_{gust}(t) = \frac{aT_{rise}}{\pi} \left[1.0 + \tanh \left(\frac{\pi(t - t_{gust})}{T_{rise}} \right) \right], \quad (3)$$

where t_{gust} is the time of the maximum acceleration and the random variables a and T_{rise} represent the acceleration and rise time respectively. Based on the probability distribution of acceleration events from the Høvsøre data, synthetic events with 50 year return period were generated and integrated in preliminary Monte-Carlo simulations. These results show that extreme accelerations have a strong impact on the ULS loads. Nevertheless, in the present case the stationary ULS cases produced highest loading and the reliability analysis proceeded with stationary ULS only.

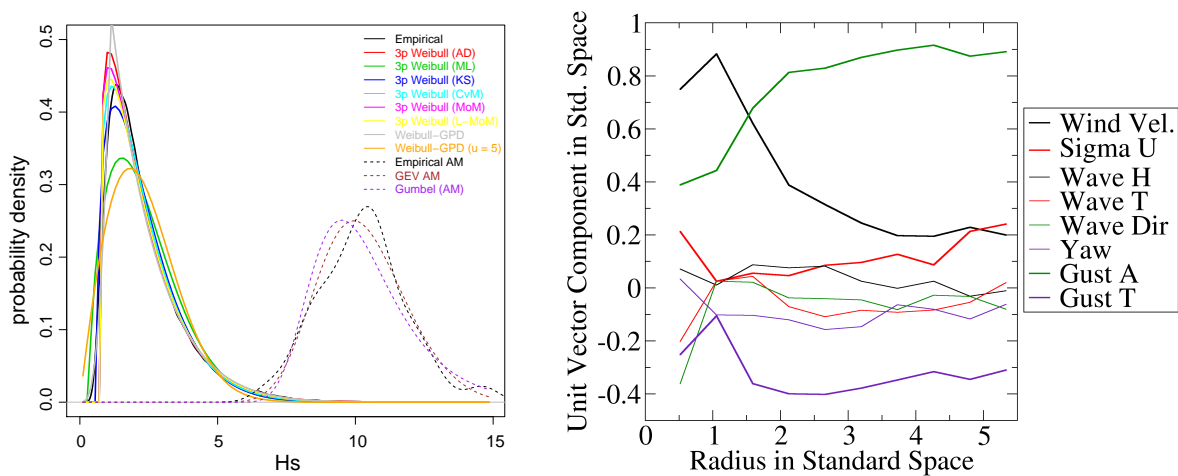


Figure 2: Illustration of uncertainties in the description of environmental conditions. Left: illustration of uncertainty in H_s distribution due to different choices of marginal probability distributions. Right: normalized input variable vector components for the largest tower bottom Von-Mises stresses at different distances (joint exceedance probabilities) in standard space, illustrating the relative contribution of environmental variables to the extreme stresses.

3.2. Model uncertainties

3.2.1. Wakes model Steady-state wake models are commonly used for wind farm production predictions during pre-design stage due to their low computational cost. However, their simplified formulations may lead to approximations. This uncertainty was evaluated on the Teesside case study by comparing wake models of the FarmShadow™ library [11] to a higher-fidelity model: the Dynamic Wake Meandering (DWM) of HAWC2 [12]. The quantity of interest is the incoming wind speed \overline{u}_{rotor} and its standard deviation $\sigma_{u_{rotor}}$. A design of experiment of simulations was computed on a 3D subspace of \mathbf{V} : free-field wind speed U , its standard deviation σ_U , and direction θ_{wind} . A Gaussian process response surface was computed for both approaches to interpolate their differences across the 3D subspace. Results reveal small overall differences in wake deficit but higher discrepancies in turbulence intensities. Notably, significant uncertainty arises when a turbine is directly downstream of others, highlighting the need for improved superposition models. More details and quantification of this model uncertainty can be found in HIPERWIND Deliverable 3.2 [13]. For the present study, wake model uncertainty did not have a direct effect on the end results (see Section 3.4).

3.2.2. Blade aerodynamics model A thorough comparison was made between conventional Blade Element Momentum (BEM) approaches using Deeplines Wind™, DIEGO, and HAWC2, and the more advanced Vortex-based model within Deeplines Wind™ [14]. Comparison was done over a 3D input space (σ_U , U and yaw angle). The outputs encompassed production, Damage Equivalent Loads (DEL) at the blade root, forces along the blades, and forces integrated over the rotor. Gaussian process interpolations were computed from design of experiments of the simulations which were iteratively enriched to provide a good estimate of the differences between BEM and Vortex for production and design outputs. It was found that outside a domain of high turbulence and wind speed, differences between BEM and Vortex remained small for this fixed-foundation case, as illustrated in Figure 3. More details can be found in [15].

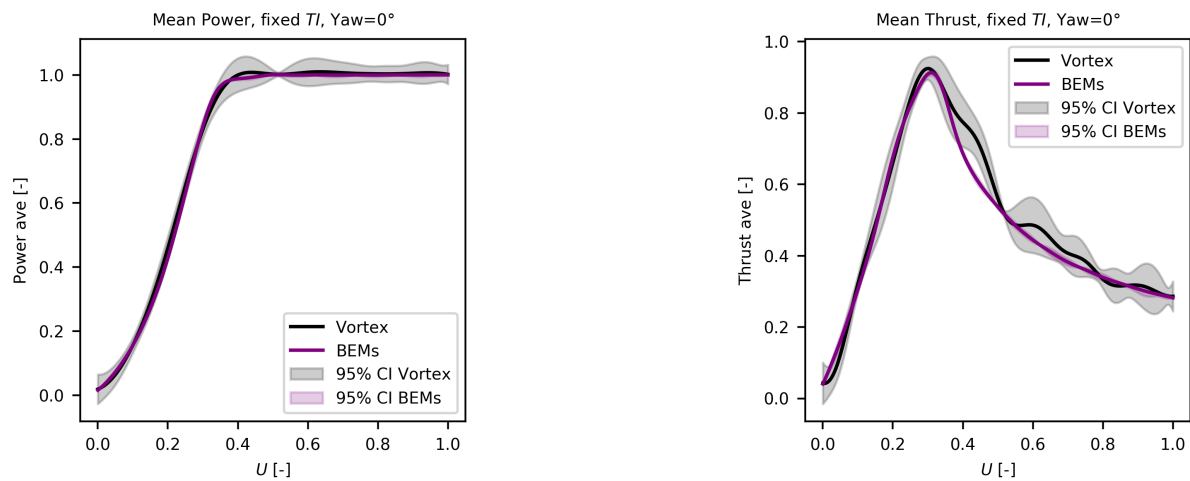


Figure 3: Normalized power and thrust time-averaged curves estimated with the metamodells for a fixed-bottom offshore wind turbine. BEMs stands for the average of BEM models.

3.2.3. Hydrodynamics model The approximation of Mac Camy & Fuchs (MCF) correction on mudline bending moment of a monopile was studied. Changing either monopile radius, water depth, wave load order or wave stretching models may produce about $\pm 10\%$ change in the Damage Equivalent Loads with some conditions for which MCF is non-conservative.

3.3. Distributions of system variables and material properties

For the material and resistance properties such as yield strength and uncertainty in the fatigue strength D_{CR} , we assume standard reference values from literature. The fatigue property distributions are based on [16]. The uncertainty in the soil stiffness is based on internal experience from EDF.

3.4. Choosing variables to include in the reliability analysis

Calculations considering wake-induced effects have indicated that wind turbines belonging to the outermost rows with maximum exposure to ambient conditions are subjected to the most significant loading. This applies to both ULS and FLS. Therefore, the FLS calculations are considering a single worst-case-scenario turbine located in the outermost row of the wind farm, without explicitly considering wake model uncertainties. Similarly for the ULS case, the ambient conditions can be considered as a worst-case reference for any wind turbine in the wind farm. The effect of aerodynamics uncertainties was also omitted as the calculations indicated that it has relatively small effects (more information can be found in [17]). The uncertainty in hydrodynamics was estimated primarily for the fatigue case, where it was found that the material (and system) uncertainties prevail, hence the latter were retained for keeping the overall problem sufficiently simple. Based on these considerations, the final choice of variables in \mathbf{U} and \mathbf{Z} was made. These variables are defined in Tables 1 and 2, for ULS and FLS respectively.

4. Reliability assessment

4.1. Ultimate limit state analysis

The ULS analysis considers extreme event scenarios with conditions that can have stationary or transient character. As also discussed in equation 1, the variability of the signals presents

Table 1: Description of variables used in the stationary ULS calculations in addition to the environmental variable vector \mathbf{V}

Group	Symbol	Description	Marginal distribution	Comment
U	θ	Yaw misalignment	Uniform ($\mu = 0, \pm 8^\circ$)	
Z	ρ	Yield strength (stress in MPa)	log-normal ($\mu = 335, \sigma = 0.1\mu$)	

Table 2: Description of variables used in the FLS calculations in addition to the environmental variable vector \mathbf{V}

Group	Symbol	Description	Marginal distribution	Comment
Z	S	Soil coefficient	Normal ($\mu = 1, \sigma = 0.2$)	Applied to the soil stiffness matrix
Z	D_{CR}	Critical damage (Miner's sum at failure)	log-normal ($\mu = 1, \sigma = 0.3$)	Cf. (JCSS, 2011)
U	θ	Yaw misalignment	Truncated Normal ($\mu = 0, \sigma = 5^\circ, -10^\circ, +10^\circ$)	Deg.
U	a	S-N curve coefficient	log-normal ($\mu = 1, \sigma = 0.3$)	

itself in both short-term scales (within a single realization), and over the long-term (i.e., during service life). The primary challenge then encompasses finding a ULS methodology exploring both the long-term and short term parametric spaces sufficiently well. This can be especially challenging with the case of small failure probabilities, where additional effort is required to achieve precise and converged results.

Several methods were compared for the stationary case in order to overcome this challenge in the most efficient way, on a simplified case study. To avoid huge computational effort at that stage, a new dynamic surrogate modelling approach was developed, based on an autoregressive model with exogenous input model (mNARX [25]). This surrogate allows to accurately predict load time series from wind turbulence input time series, replacing aero-servo-hydro-elastic simulations. From the results of this comparison, the sequential sampling strategy introduced in [20] was selected as most feasible ULS approach for a realistic case study. It computes the short term probability of failure given the long term by fitting a Generalized-Extreme-Value (GEV) distribution of maximum output. Kriging is then used to extrapolate the GEV parameters for integrating the failure probability over long-term space. New simulations are computed iteratively only at regions found important to evaluate the ULS. The resulting computations effort is thus optimized for a given accuracy on failure probability estimate. The left hand side of figure 4 illustrates the iterative enrichment of Design of Experiments by this method. Here, 7000 simulations were needed to obtain a sufficiently accurate failure probability estimation (5 iterations of 70 long-term points and for each long-term configuration 20 random seeds are used to fit the GEV distribution).

For the transient case, the short term variation is not so important since the failure is mainly driven by the occurrence of gust events which can be described by few parameters. Thus, classical reliability methods in small dimension (see [18]) can be applied.

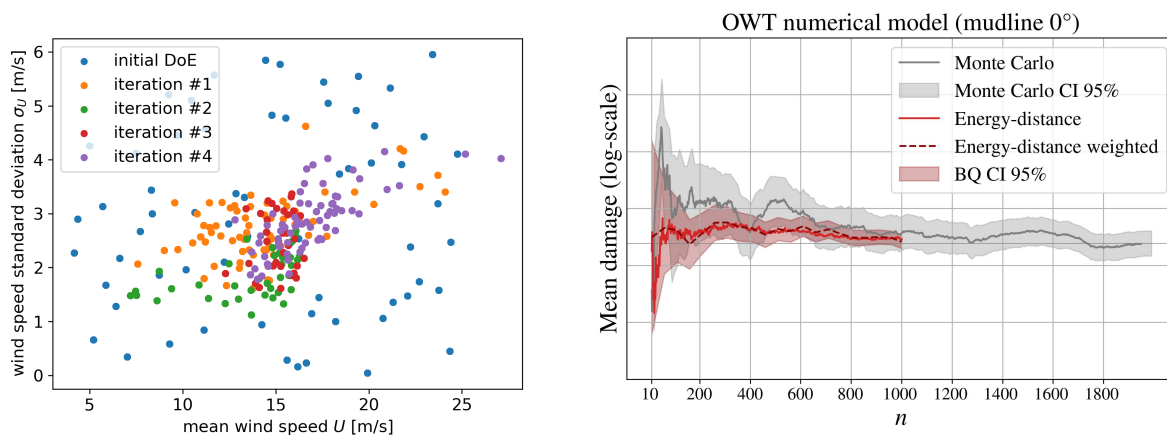


Figure 4: Left: points of simulations required by the sequential sampling approach in mean wind speed vs turbulence space. Right: Convergence of the proposed sampling methodologies for FLS, compared to standard Monte Carlo sampling.

4.2. Fatigue limit state analysis

Fatigue damage accumulates over time, meaning that in the FLS case the probability of failure increases with time, and p_f is defined as the annual probability of failure of the structure at the last year of its intended lifetime. Particular challenges with the FLS approach included 1) the need to integrate over the distribution of \mathbf{V} at each limit state evaluation, which effectively introduces a double numerical integration loop (as the reliability computation itself is a numerical integration problem), and 2) the presence of system variables \mathbf{Z} which alter the system dynamic behavior at each iteration. The latter makes it impossible to use simple efficient solutions such as mapping the system behavior with a surrogate model. The possible solutions are computationally demanding: either to recompute the dynamic behavior of the system at each iteration with a full-fidelity model, or train a highly complex surrogate model which also maps the variables in \mathbf{Z} . These considerations drove the choice of reliability assessment methods towards maximum sampling efficiency while still using the full-fidelity aeroelastic model at each reliability iteration. As a result we used a flexible and efficient method, called “kernel-herding”, to perform given-data uncertainty propagation for probabilistic fatigue assessment (i.e., directly subsampling from environmental data without inferring a probabilistic model).

Preliminary evaluations were performed for D_{global} under varying values of the \mathbf{U} variables. The distribution of D_{global} in this analysis shows a central part (mode) roughly between 10^{-4} and 10^{-3} . Consequently, failures probabilities are low. Using the reference D_{CR} log-normal distribution, the failure probability p_f is about 10^{-13} . P_f is highly sensitive to this D_{CR} distribution assumption. When considering a positive truncated normal distribution instead, P_f becomes much higher (about 10^{-6}). However, it remains lower than the 10^{-4} probability threshold sometimes considered in the literature. A robustness analysis on the variable distribution parameters confirms that the FLS reliability is mostly driven by D_{CR} .

4.3. Design utilization study

Ideally, optimal design under uncertainty can be obtained by Reliability-Based Design Optimization (RBDO). Due to the high computational cost of this approach, we apply a simplification which under certain conditions allows us to obtain an improved design closer to the target reliability in just a few iterations.

We employ a series of design evaluations, starting with the nominal design parameters of

the turbines at the Teesside wind farm. A set of simulations from the IEC-61400-3 [22] design basis are computed for a single turbine. The results are used to identify the most critical limit states, in this case the maximum Von Mises stress σ_{VM} at the monopile basis for stationary ULS in a case with non-operational turbine. Assuming a beam formulation for the tower and the monopile, σ_{VM} can be derived from the global moment M and vertical force due to the weight of above part F_z as a function of the external diameter D and thickness t :

$$\sigma_{VM} = M \frac{64}{\pi (D^4 - (D - 2t)^4)} + F_z \frac{4}{\pi (D^2 - (D - 2t)^2)}. \quad (4)$$

The annual failure probability of the nominal design for that limit state is estimated with the procedure described in section 4.1 and the uncertain variables listed in Table 1 - resulting in annual failure probability in the order of $P_f \approx 10^{-13}$, indicating a significant amount of conservatism which can be explained both by non site-specific loading and deterministic design with large safety factors.

As a next step, the design parameters are modified in order to reduce the material capacity and obtain reliability which is closer to the target annual $P_{f,target} = 5 \times 10^{-4}$. We found that when reducing the thickness by up to 25%, the changes in M are small enough to assume its maximum to be constant with respect to design changes, while the contribution of F_z to σ_{VM} is much smaller than that of M . Taking advantage of this crucial simplification, we can compute the new design as the solution of an optimisation reducing t , under the following constraints: D/t is unchanged to ensure manufacturability of the solution, natural frequencies of the structure are farther than 10% from the 3P frequency, monopile basis plastic failure probability is less than 10^{-4} , shell and beam buckling (same criteria than in WISDEM software of NREL) are avoided.

Note that the failure probability during this optimization uses the constant-bending moment assumption to update σ_{VM} with D and t change, using the same simulations than for the initial design reliability estimate.

The solution found led to a mass reduction of 21% with the tower resonance as limiting criterion. The failure probability of monopile basis plasticity was evaluated more accurately with new simulations according to the procedure from section 4.1, and was found to be in the order of $P_f \approx 10^{-9}$. Compared to the original design, this is four orders of magnitude closer to the target reliability, and further adjustment of the design was not possible due to the resonance constraints becoming active.

5. Conclusions

The present study demonstrated the process of incorporating uncertainties in wind turbine design, by showing a practical application to an offshore wind farm. Our main conclusions are:

- Use of an integrated modelling approach where the entire support structure system (tower & foundation) is considered, together with accurate detailed modelling of the environmental conditions, can lead to significant savings compared to the classical design process that has been used in early offshore wind farms.
- A clear benefit of taking uncertainty into account is that the impact of taking specific modelling choices can be evaluated, and the best modelling options can be selected. This ultimately leads to design improvements.
- Probabilistic design remains a challenge due to its high complexity and often insufficient information to guide the choices of variables, distributions, and analysis methods.
- The potential of reducing conservatism can be evaluated with design utilization studies as presented in this work. It was also discussed that in some cases, certain simplifying assumptions can greatly facilitate this process.

Acknowledgements

This work is supported by the Hiperwind project funded through the EU Horizon 2020 research program, Grant Agreement 101006689. Thanks to G. Huwart and N. Bonfils from IFPEN for contribution to the multiscale model chain, to S. Eldevik and C. Ferreira for kriging estimate of model uncertainty, and for B. Jezequel in estimating probabilistic loading in the farm.

References

- [1] International Electrotechnical Committee (2023) IEC TS 61400-9 ED1: Wind energy generation systems – Part 9: Probabilistic design measures for wind turbines.
- [2] HIPERWIND: Highly advanced Probabilistic design and Enhanced Reliability methods for high-value, cost-efficient offshore wind. A research project funded by the EU Horizon2020 program. www.hiperwind.eu
- [3] International Electrotechnical Committee (2019) IEC International Standard 61400-1 ED4: Wind energy generation systems – Part 1: Design requirements.
- [4] Madsen, H. O., Krenk, S., and Lind, N. C. (2006). *Methods of Structural Safety*. (2 ed.) Dover Publications.
- [5] N. Dimitrov, M. Pedersen, Á. Hannesdóttir(2024). An open-source Python-based tool for Mann turbulence generation with constraints and non-Gaussian capabilities *Journal of Physics: Conference Series*, *submitted*.
- [6] M. McWilliam, N. Bonfils, N. Dimitrov, S. Dou (2022) *Wind farm parameterization and turbulent wind box generation*, *HIPERWIND Deliverable no: D3.1*
- [7] M. Kelly and E. Vanem (2022) *Environmental joint probability distributions and uncertainties*, *HIPERWIND Deliverable no: D2.3*
- [8] M. Kelly, 2024. Flow acceleration statistics: a new paradigm for wind-driven loads, towards probabilistic turbine design. *Wind Energy Science*, under submission.
- [9] M. Bakhoday Paskyabi, H. Bui, and M. Mohammadpour Penchah, *Atmospheric-Wave Multi-Scale Flow Modelling*, *HIPERWIND Deliverable no: D2.1*.
- [10] X. Ning, and M. Bakhoday Paskyabi, H. Bui, M. M Penchah. 2023. Evaluation of sea surface roughness parameterization in meso-to-micro-scale simulation of the offshore wind field. *Atmospheric Research*.
- [11] F. Blondel. 2023. Brief communication: A momentum-conserving superposition method applied to the super-Gaussian wind turbine wake model. *Wind Energy Science*, 8(2), 141-147.
- [12] I. Reinwardt et al. (2021) Validation of the dynamic wake meandering model with respect to loads and power production. *Wind Energy Science*, 6(2), 441-460.
- [13] E. Ardillon et al. (2022) *Turbine loading and wake model uncertainty*, *HIPERWIND Deliverable no: D3.2*.
- [14] F. Blondel, PA. Joulin, C. Le Guern (2024) Towards vortex-based wind turbine design using GPUs and wake accommodation. *Journal of Physics: Conference Series*, *submitted*.
- [15] C. Peyrard et al. (2022). *Aero-servo-hydroelastic model uncertainty*, *HIPERWIND Deliverable no: D3.3*.
- [16] Joint Committee of Structural Safety (2011) JCSS Probabilistic Model Code, Part 3: resistance models – Fatigue models for metallic structures
- [17] M. Guiton et al. (2023) Uncertainties in loads on offshore wind turbine: learnings from HIPERWIND H2020 project. In: proceedings of the SEANERGY 2023 conference, Paris, France.
- [18] J.M. Bourinet. 2018. Reliability analysis and optimal design under uncertainty-Focus on adaptive surrogate-based approaches. *HDR*.
- [19] Y. Chen and M. Welling and A. Smola. 2010. Super-samples from kernel herding. *Proceedings of the Twenty-Sixth Conference on Uncertainty in Artificial Intelligence*. 109 – 116.
- [20] O. Gramstad et al. 2020. Sequential sampling method using Gaussian process regression for estimating extreme structural response. *Marine Structures*. **72**. 102780.
- [21] Müller, K. and Cheng, P.W. 2018. Application of a Monte Carlo procedure for probabilistic fatigue design of floating offshore wind turbines. *Wind Energy Science*. **3**. 149 – 162.
- [22] International Electrotechnical Committee (2019) IEC International Standard 61400-3: Wind energy generation systems – Part 3-1: Design requirements for fixed offshore wind turbines.
- [23] Vanem, E, Fekhari, E, Dimitrov, N, Kelly, M, Cousin, A, Guiton, M 2023 *Proc. 42st International Conference on Ocean, Offshore and Arctic Engineering (OMAE 2023)*
- [24] Vanem, E. and Fekhari, E. and Dimitrov, N. and Kelly, M. and Cousin, A. and Guiton, M. 2024 A Joint Probability Distribution for Multivariate Wind-Wave Conditions and Discussions on Uncertainties *Journal of Offshore Mechanics and Arctic Engineering*, **146**(6), 061701.
- [25] Schär, S., Marelli, S. and Sudret, B. 2024. Emulating the dynamics of complex systems using autoregressive models on manifolds (mNARX). *Mechanical Systems and Signal Processing*. **208**. 110956.